

2.4 μm cutoff wavelength avalanche photodiode on InP substrate

R. Sidhu, L. Zhang, N. Tan, N. Duan, J.C. Campbell, A.L. Holmes, Jr., C.-F. Hsu and M.A. Itzler

An InP-based avalanche photodiode with a cutoff wavelength of 2.4 μm is reported. Type-II GaInAs-GaAsSb quantum wells lattice-matched to InP were used in the absorption region of the photodiode for long-wavelength absorption. The device exhibited multiplication gain in excess of 30 at room temperature and in excess of 200 at 225 Kelvin with dark current density near breakdown of less than 0.66 mA/cm².

Photodiodes operating in the mid-wave infrared (2–5 μm) wavelength region find many applications in remote sensing, medical diagnostics, thermal imaging and chemical sensing. Performance requirements for these applications include high sensitivity, high speed, near room-temperature operation, good uniformity, and high yield. Avalanche photodiodes (APDs) can achieve 5–10 dB higher sensitivities compared to *pin* photodiodes because of their internal multiplication gain. At present, HgCdTe is the predominant material system used for mid-wave infrared (MWIR) photodiodes [1]. Avalanche photodiodes fabricated from HgCdTe exhibit very low multiplication noise [2]. However, HgCdTe focal plane arrays used for imaging applications often suffer from material non-uniformity and low yield [3]. This has led to research efforts to explore alternative material systems to make devices for the applications listed above. We have recently reported a *pin* photodiode on InP substrate with a cutoff wavelength of 2.39 μm [4]. In this Letter, we report an InP-based long-wavelength avalanche photodiode, using lattice-matched Ga_{0.47}In_{0.53}As-GaAs_{0.51}Sb_{0.49} type-II quantum wells for absorption.

Separating the narrow-bandgap absorption region in an APD from the wide-bandgap multiplication region by a thin field-control charge region allows high electric field in the multiplication region while maintaining low electric field in the absorption region [5]. Thus, in the separate absorption, charge, and multiplication (SACM) structure, high multiplication gains can be achieved while maintaining low dark current. The SACM structure also leads to low multiplication noise by injecting only one type of charge-carrier into the multiplication region. In the APD reported in this Letter, holes are injected from the absorption region into the InP multiplication region.

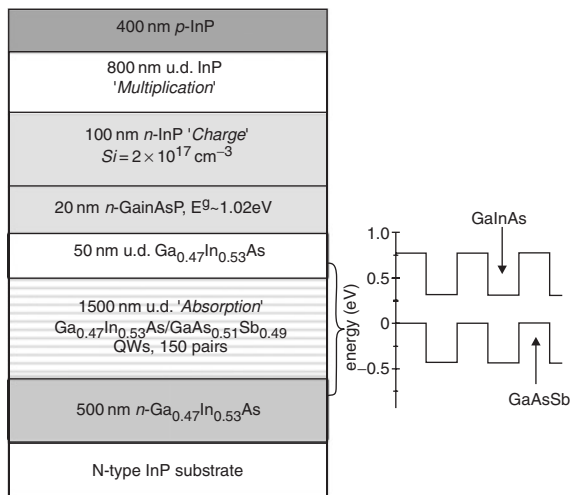


Fig. 1 Schematic device structure and band line-up between Ga_{0.47}In_{0.53}As and GaAs_{0.51}Sb_{0.49}

A schematic of the device structure and the band line-up of the type-II QWs are shown in Fig. 1. The device was grown in a Varian Gen-II molecular beam epitaxy (MBE) chamber equipped with standard group-III effusion cells and Veeco valved crackers for As and Sb. Material composition and layer thicknesses were verified using high resolution X-ray diffraction. Details of GaAsSb MBE growth have been reported in [6]. The wafers were fabricated into top-illuminated mesa structures using a H₃PO₄:H₂O₂:H₂O (1:1:10) wet-chemical etch. The mesas were then passivated by plasma-enhanced chemical vapour

deposition of 2000 Å of SiO₂. Ti-Pt-Au metal ring contacts were deposited on the top p-surface of the mesa, and AuGe-Ni-Au contacts were deposited on the n-surface. Conventional photolithography and lift-off metallisation techniques were used to define the metal contacts. Microwave contact pads were fabricated for wire bonding.

Reverse current-voltage characteristics at different temperatures are shown in Fig. 2. Room-temperature dark current at punchthrough (–37 V) is 130 nA for a 44 μm -diameter device. The dark current drops rapidly with temperature, and at 225 K, the dark current at 90% of breakdown is approximately 10 nA, corresponding to current density of 0.66 mA/cm². Photocurrent and dark current data from a 44 μm -diameter device at room temperature and 225 K are plotted in Figs. 3a and b, respectively. It can be seen from the slope of the photo-response that there is avalanche gain at punchthrough. This gain at punchthrough was determined by comparing the photocurrent from a 64 μm -diameter APD biased at –37 V to the photocurrent of a *pin* device of the same size, under the same illumination from a 1.55 μm wavelength laser. The laser light was focused to a 10 μm -diameter spot. The *pin* photodiode had the same absorption region, and was biased at low voltage to ensure unity gain. The ratio of the photocurrents at room temperature was 1.7, which was assumed to be the gain of the APD at –37 V. The gain curves against bias voltage are also plotted in Figs. 3a and b.

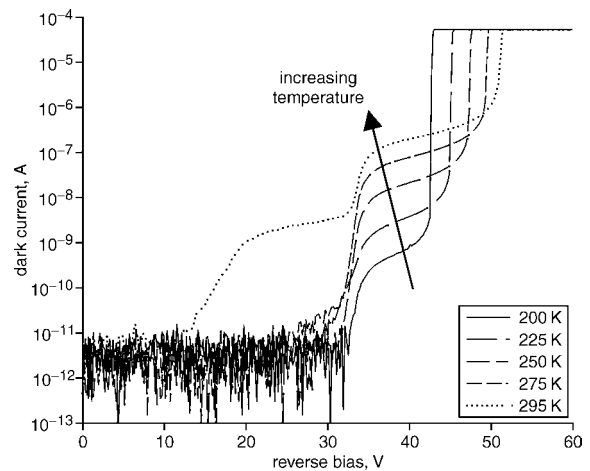


Fig. 2 Dark current against reverse bias voltage from 44 μm -diameter device, measured at 200, 225, 250, 275, 295 K

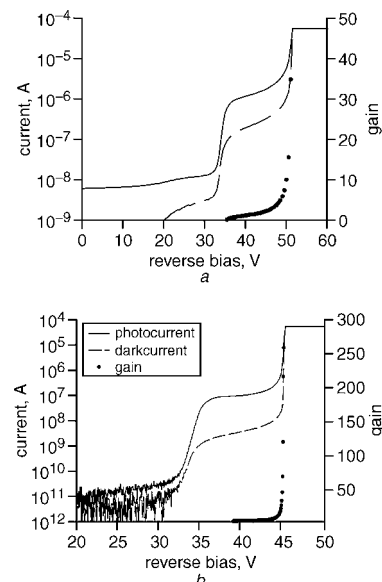


Fig. 3 Reverse *I*–*V* and gain at room temperature and at 225 K
a Room temperature
b 225 K

A Nicolet Magna-II FTIR spectrometer with an SRS 570 low-noise current preamplifier was used to measure the spectral response at different temperatures and bias conditions. The normal incidence

photo-response spectra measured at various temperatures at -37 V reverse bias are shown in Fig. 4a. The measured data at each temperature was normalised to the peak value at that temperature. These peak values were from the type-I (spatially direct) peaks from $\text{Ga}_{0.47}\text{In}_{0.53}\text{As}$ and $\text{GaAs}_{0.51}\text{Sb}_{0.49}$ QWs at about $1.5\ \mu\text{m}$ (not shown in the Figure.) The type-II (spatially indirect) response from 1.8 to $2.5\ \mu\text{m}$ is shown in the Figure. The photo-response data from the FTIR was calibrated using a PbS detector with known responsivity, and verified using a second calibrated long-wavelength GaInAs detector. As expected, the photo-response red-shifts with increase in temperature, because of the reduction of the bandgaps at higher temperature. The relative response (and responsivity) increases with temperature. We believe that this is due to photo-generated carriers having more energy to escape the QWs and transit to the electrodes. Room-temperature spectral response measured at different reverse bias voltages showed a change in the shape of the response curve. Further investigation is under way to understand the relation between electric field across the absorption region and the shape of the optical-response.

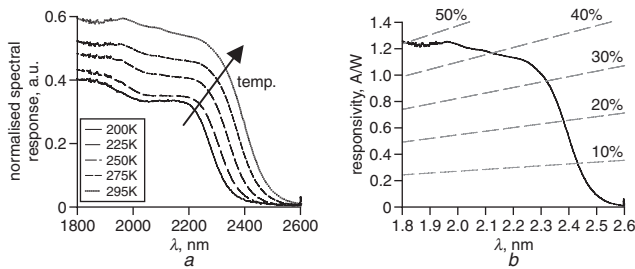


Fig. 4 Normal incidence photo-response at different temperatures, and room-temperature responsivity measured at -37 V bias

a Normal incidence photo-response at different temperatures

b Room-temperature responsivity measured at -37 V bias

Diagonal lines (dashed) show equivalent unity gain external quantum efficiency

Responsivity of this device was measured as described in [4]. Room-temperature responsivity of the device at -37 V is shown in Fig. 4b. The diagonal lines in the graph represent equivalent unity gain external quantum efficiency.

Multiplication gain at a given electric field has temperature dependence because of the change in electron and hole ionisation coefficients with temperature. The gain at different temperatures was determined by comparing the responsivity of the APD at that temperature to the responsivity of the *pin* device measured at the same temperature. Even though the two photodiodes had similar absorption regions, their responsivity curves have slightly different shapes. Thus some error is introduced in the determination of gain by this method.

As stated earlier, this device had a coating of $2000\ \text{\AA}$ of SiO_2 on the top surface, which results in approximately 20% back reflection of 2 to $2.5\ \mu\text{m}$ wavelength incident light. An antireflection (AR) coating can increase the responsivity and quantum efficiency of the device, as reported in [4].

Conclusion: We have demonstrated an InP-based avalanche photodiode with response up to $2.4\ \mu\text{m}$, using $\text{Ga}_{0.47}\text{In}_{0.53}\text{As}$ - $\text{GaAs}_{0.51}\text{Sb}_{0.49}$ type-II quantum wells. The device achieved room-temperature gain in excess of 30 and had type-II room-temperature external quantum efficiency of 38% at $2.2\ \mu\text{m}$. This is the first reported InP-based avalanche photodiode with response past $2\ \mu\text{m}$.

Acknowledgment: This work is supported by the Air Force Office of Scientific Research under Contract FA9550-05-C-0007.

© IEE 2006

27 September 2005

Electronics Letters online no: 20063415

doi: 10.1049/el:20063415

R. Sidhu, L. Zhang, N. Tan, N. Duan, J.C. Campbell and A.L. Holmes, Jr. (Microelectronics Research Center, Electrical and Computer Engineering Department, The University of Texas at Austin, R9900, 1 University Station, Austin, TX, 78712, USA)

E-mail: holmes@mail.utexas.edu

C.-F. Hsu and M.A. Itzler (Princeton Lightwave Inc., 2555 Route 130 South, Cranbury, NJ 08512, USA)

References

- 1 Zandian, M., *et al.*: 'Mid-wavelength infrared p-on-n $\text{Hg}_{1-x}\text{Cd}_x\text{Te}$ heterostructure detectors: 30–120 Kelvin state-of-the-art performance', *J. Electron. Mater.*, 2003, **32**, (7), pp. 803–809
- 2 Norton, P.: 'HgCdTe infrared detectors', *Opto-Electron. Rev.*, 2002, **10**, (3), pp. 159–174
- 3 Phillips, J.D., *et al.*: 'Uniformity of optical absorption in HgCdTe epilayer measured by infrared spectromicroscopy', *Appl. Phys. Lett.*, 2003, **83**, pp. 3701–3703
- 4 Sidhu, R., *et al.*: 'A long-wavelength photodiode on InP using lattice-matched GaInAs-GaAsSb type-II quantum wells', *IEEE Photonics Technol. Lett.*, 2005, **17**, (12), pp. 2715–2717
- 5 Anselm, K.A., *et al.*: 'Performance of thin separate absorption, charge, and multiplication avalanche photodiodes', *IEEE J. Quantum Electron.*, 1998, **34**, pp. 482–490
- 6 Sun, X., *et al.*: 'GaAsSb: a novel material for near infrared photodetectors on GaAs substrates', *IEEE J. Sel. Top. Quantum Electron.*, 2002, **8**, (4), pp. 817–822